

## Article

# Prediction Model for Random Variation in FinFET Induced by Line-Edge-Roughness (LER)

Jinwoong Lee <sup>1</sup>, Taeon Park <sup>1</sup>, Hongjoon Ahn <sup>2</sup>, Jihwan Kwak <sup>3</sup>, Taesup Moon <sup>1,2,\*</sup> and Changhwan Shin <sup>1,\*</sup>

<sup>1</sup> Department of Electrical and Computer Engineering, Sungkyunkwan University, Suwon 16419, Korea; leejuw421@gmail.com (J.L.); pte1236@skku.edu (T.P.)

<sup>2</sup> Department of Artificial Intelligence, Sungkyunkwan University, Suwon 16419, Korea; hong0805@skku.edu

<sup>3</sup> Department of Electronic and Electrical Engineering, Sungkyunkwan University, Suwon 16419, Korea; jihwan0508@skku.edu

\* Correspondence: tsmoon@skku.edu (T.M.); cshin@skku.edu (C.S.); Tel.: +82-31-290-7694 (C.S.)

**Abstract:** As the physical size of MOSFET has been aggressively scaled-down, the impact of process-induced random variation (RV) should be considered as one of the device design considerations of MOSFET. In this work, an artificial neural network (ANN) model is developed to investigate the effect of line-edge roughness (LER)-induced random variation on the input/output transfer characteristics (e.g., off-state leakage current ( $I_{off}$ ), subthreshold slope ( $SS$ ), saturation drain current ( $I_{d,sat}$ ), linear drain current ( $I_{d,lin}$ ), saturation threshold voltage ( $V_{th,sat}$ ), and linear threshold voltage ( $V_{th,lin}$ )) of 5 nm FinFET. Hence, the prediction model was divided into two phases, i.e., “Predict  $V_{th}$ ” and “Model  $V_{th}$ ”. In the former, LER profiles were only used as training input features, and two threshold voltages (i.e.,  $V_{th,sat}$  and  $V_{th,lin}$ ) were target variables. In the latter, however, LER profiles and the two threshold voltages were used as training input features. The final prediction was then made by feeding the output of the first model to the input of the second model. The developed models were quantitatively evaluated by the Earth Mover Distance (EMD) between the target variables from the TCAD simulation tool and the predicted variables of the ANN model, and we confirm both the prediction accuracy and time-efficiency of our model.

**Keywords:** line-edge roughness (LER); random variation; machine learning; artificial neural network



**Citation:** Lee, J.; Park, T.; Ahn, H.; Kwak, J.; Moon, T.; Shin, C. Prediction Model for Random Variation in FinFET Induced by Line-Edge-Roughness (LER). *Electronics* **2021**, *10*, 455. <https://doi.org/10.3390/electronics10040455>

Academic Editor: Ray-Hua Horng  
Received: 11 January 2021  
Accepted: 9 February 2021  
Published: 12 February 2021

**Publisher's Note:** MDPI stays neutral with regard to jurisdictional claims in published maps and institutional affiliations.



**Copyright:** © 2021 by the authors. Licensee MDPI, Basel, Switzerland. This article is an open access article distributed under the terms and conditions of the Creative Commons Attribution (CC BY) license (<https://creativecommons.org/licenses/by/4.0/>).

## 1. Introduction

In the past few decades, the physical dimension of metal oxide semiconductor field-effect transistor (MOSFET) has been dramatically decreased not only to increase the number of transistors in integrated circuits (ICs) but also to boost up the performance of transistor in ICs. As of 2020, a few billion transistors are integrated into a single piece of IC chip. However, the process-induced random variation should be considered when designing and integrating transistors in IC. It is known that the process-induced random variation is primarily occurred by three root-causes, i.e., line edge roughness (LER) [1], random dopant fluctuation (RDF) [2], and work function variation (WFV) [3].

With the machine learning (ML) technique, the impact of LER-induced random variation in 5 nm FinFET is quantitatively predicted (i.e., major points in the input transfer characteristic of 5 nm FinFET (drain current- vs.-gate voltage ( $I_d$ - $V_g$ ) curve) are predicted). The major causes of LER are originated from photolithography process: (1) the line edge along the photoresist pattern is determined by the intensity of light exposure. Due to the uneven intensity, the line edge should be rough in nature. (2) Acid cations (which are generated in the deprotection process) affect the mask pattern, resulting in LER [4–6]. The LER profile can be characterized (and can be reconfigured) with three parameters, i.e., RMS amplitude ( $\sigma$ ), correlation length ( $\xi$ ), and roughness exponent ( $\alpha$ ) [7–11]. In Figure 1, an exemplary LER profile is illustrated. The RMS amplitude indicates the standard deviation of roughness along the line of the pattern. The correlation length means the “average”

value of the physical distance in-between peak and valley. Note that two correlation lengths in  $x$ -/ $y$ -directions are necessary to characterize a surface roughness. In three-dimensional device structure, e.g., FinFET, two correlation lengths, i.e.,  $x$  and  $y$ , are used together to reconfigure the surface roughness of sidewall in FinFET. The roughness exponent is defined as a fractal dimension. More specifically, this indicates the amount of high-frequency components left behind in LER profile [5,12,13]. Figure 2 shows the unexpected variation of FinFET's Id–Vg curves caused by LER. In Figure 2a, the red-colored line indicates the Id–Vg curve of nominal FinFET without LER, and the gray-colored lines show Id–Vg curves of 250 FinFETs with identical LER profiles. Figure 2b shows the Id–Vg curves of FinFETs with two LER profile combinations (note that 250 cases are sampled for each case). The gray-colored lines have  $\sigma$ : 0.7295,  $\xi_x$ : 89.3916,  $\xi_y$ : 195.6248, and the dark gray-colored lines have  $\sigma$ : 0.1411,  $\xi_x$ : 96.7100,  $\xi_y$ : 186.6837. This shows that the larger the amplitude is, the larger the variation is.

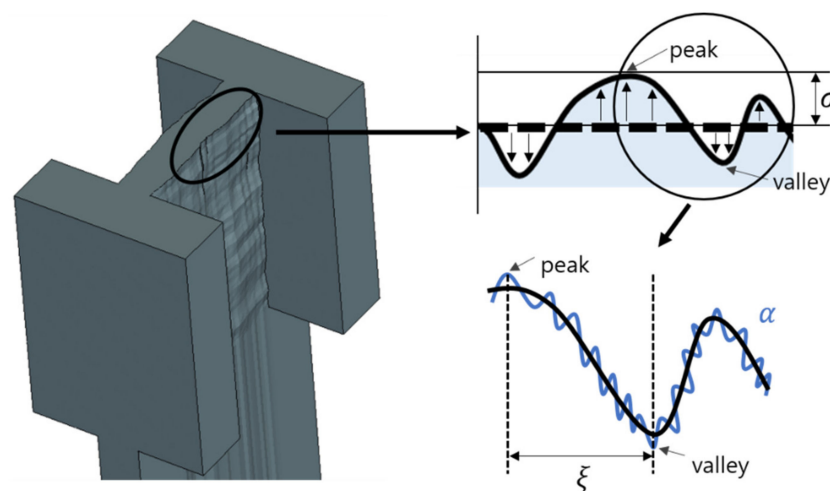


**Figure 1.** A line-edge roughness (LER) profile can be characterized with three key features such as rms amplitude ( $\sigma$ ), correlation length ( $\xi$ ), and roughness exponent ( $\alpha$ ).

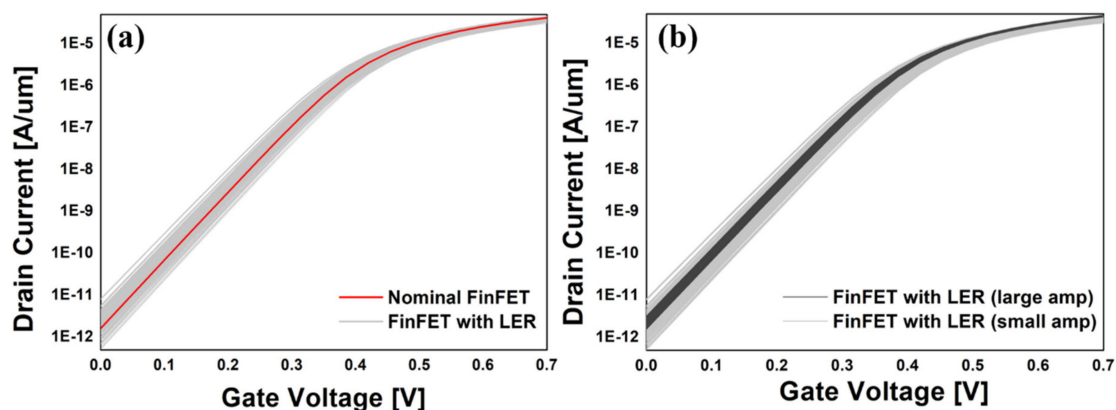


**Figure 2.** (a) Drain current- vs.-gate voltage (Id–Vg) curves of FinFET with LER vs. nominal FinFET. (b) Id–Vg curves of FinFET with LER but with different amplitudes.

In the past few years, many studies on LER-induced random variations have been done. The typical method to evaluate the effect of LER-induced random variation on FinFET device is simply to run the Technology Computer-Aided Design (TCAD) simulations with additional in-house software to implement LER [14]. However, TCAD simulations spend tens of minutes (up to hours or even days) because the total number of device-under-test should be more than a few hundred to obtain statistically significant data. In this work, to aggressively shorten the long simulation running time, an artificial neural network

(ANN) is proposed and developed. We set the LER profiles as a training input feature and specify the characteristic parameters of Id–Vg curve of the device as target variables, so that perceptrons in each layer of the ANN model can learn the coefficient between them. If there is a model (which has been trained with various LER profiles), it can predict the fluctuation of Id–Vg curve within seconds.

## 2. Simulation

When training a machine learning (ML) model, it is necessary to prepare both training-data and test-data. In this work, those data sets were generated and obtained using TCAD (Sentaurus) and MATLAB tools. A nominal 5 nm FinFET device was designed, and it is the nominal object for the ML model. Note that the device design parameters for 5 nm FinFET device are summarized in Table 1. The quasi-atomistic model with the 2-D autocorrelation function (ACVF) method [14] (see Equation (1) below) was used to design and reconfigure the LER on the sidewall of FinFET. When creating the LER profiles, the features for the LER profiles were uniformly sampled within a limited range. Note that the range of LER profiles are as follows:  $\sigma$  from 0.1 nm to 0.8 nm,  $\xi_x$  from 10 nm to 100 nm,  $\xi_y$  from 20 nm to 200 nm.

$$ACVF(x, y) = \sigma^2 \exp \left[ - \left\{ - \left( \frac{(x \cos \theta + y \sin \theta)^2}{\xi_x^2} + \frac{(-x \sin \theta + y \cos \theta)^2}{\xi_y^2} \right)^{\frac{1}{2}} \right\} \right]. \quad (1)$$

**Table 1.** Device design parameters of the FinFET used in this work.

Device Parameters			
Symbol	Description	Unit	Value
$L_g$	Gate length	nm	20
$T_{ox}$	Equivalent oxide thickness (HfO <sub>2</sub> )	nm	0.3
$W_{fin}$	Fin width	nm	7
$H_{fin}$	Fin height	nm	50
$V_{DD}$	Power supply voltage	V	0.7
$I_{Vti}$	Constant current	A/um	$5.35 \times 10^{-7}$
$\sigma$	RMS amplitude	nm	0.1~0.8
$\xi_x$	$x$ -axis correlation length	nm	10~100
$\xi_y$	$y$ -axis correlation length	nm	20~200

For three different LER profiles, the input transfer characteristics (i.e., Id–Vg curve) of FinFET were investigated. To investigate the impact of LER profiles on the Id–Vg characteristic of FinFET, 150 training data sets for various LER profiles were prepared (Note that a single training data set consists of 50 Id–Vg curves). We extracted 10 test data sets (consisting of 250 Id–Vg curves) out of 150 training data sets to verify the prediction model.

All data sets consist of both LER profiles (e.g., RMS amplitude ( $\sigma$ ),  $x$ -axis correlation length ( $\xi_x$ ), and  $y$ -axis correlation length ( $\xi_y$ )) and the Id–Vg curve's characteristic parameters (e.g., off-state leakage current ( $I_{off}$ ), subthreshold slope ( $SS$ ), the saturation drain current ( $I_{d,sat}$ ), the linear drain current ( $I_{d,lin}$ ), the saturation threshold voltage ( $V_{th,sat}$ ), and linear threshold voltage ( $V_{th,lin}$ )). The scale of each data in the dataset was different from that of the other data. For example, in a test-data set, the mean of  $I_{off}$  is 7.37 pA, but the mean of  $V_{th}$  is 299 mV. To address this issue as well as to achieve a superior learning performance, it is mandatory to have an identical scale for all the data. In the ML society, there are a few methods available for data scaling. In this work, the “Robust Scaling” method was adopted and used, because the impact of outliers on the learning performance can become minimal with the method [15].

$$SS = \frac{1000(V_{th} - V_{off})}{\log_{10}(I_{V_{th}}/I_{V_{off}})} \quad (2)$$

The subthreshold features (i.e.,  $I_{off}$ ,  $V_{th}$ , and  $SS$ ) (which are the three parameters among the six Id–Vg characteristic parameters) are physically and mathematically associated with each other (see Equation (2)). To improve the performance of the prediction model, we divided the model into two phases: (1) Predict  $V_{th}$ , predicting  $V_{th}$  using the LER profiles, and (2) Model  $V_{th}$ , using the LER profiles and  $V_{th}$  as training input features to train the coefficient of Equation (2). Figure 3 shows the overview of the prediction model.

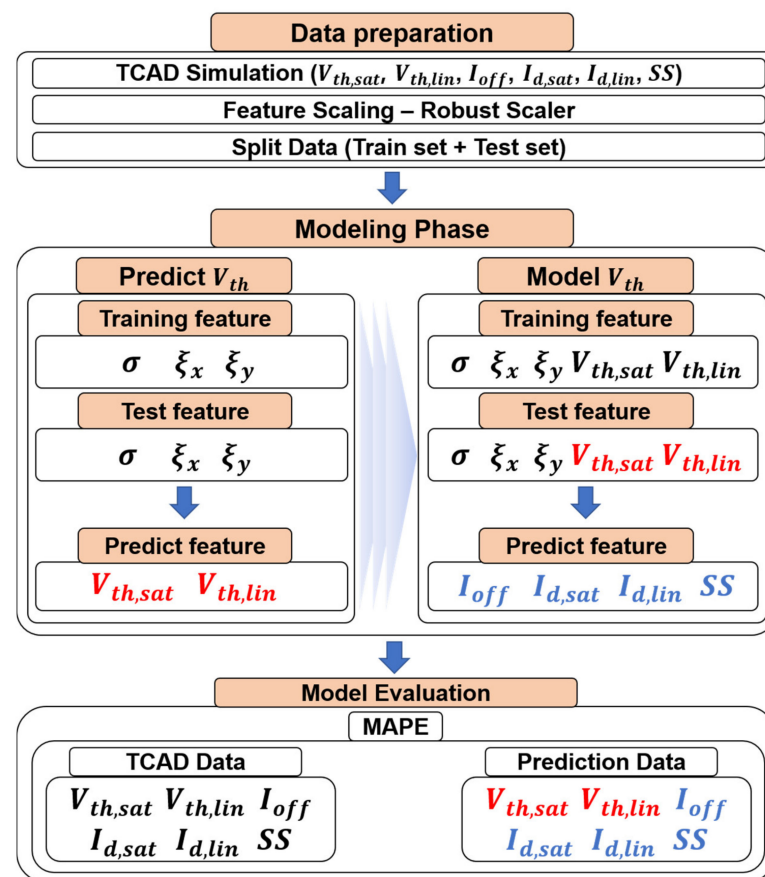
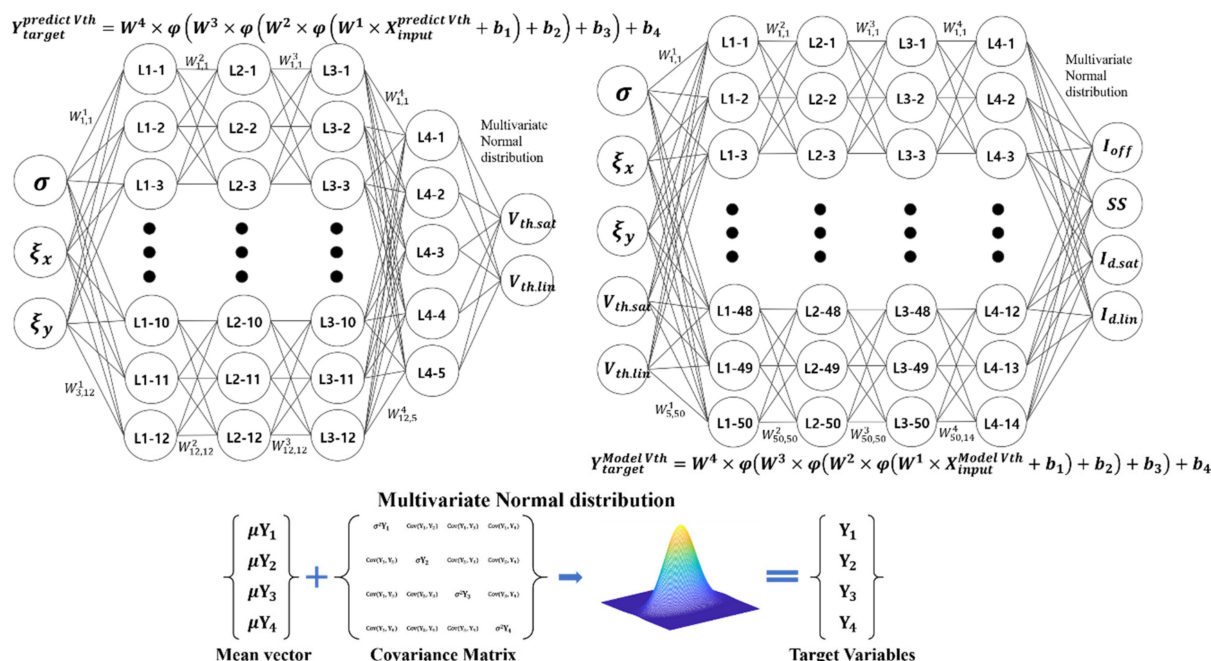


Figure 3. Overview of the prediction model.

Figure 4 shows the conceptual diagram of two artificial neural networks (ANN): (1) Predict  $V_{th}$  and (2) Model  $V_{th}$ . The input features of Model  $V_{th}$  are (1) 3 features for LER profiles and (2) 2 features of  $V_{th,sat}$  and  $V_{th,lin}$  (in total, 5 features). The target variables of Model  $V_{th}$  are the characteristic parameters of Id–Vg curve excluding  $V_{th,sat}$  and  $V_{th,lin}$ .

It is known that the LER-induced threshold voltage variation in various types of field-effect transistor follows the Gaussian distribution [1,16,17]. Based on those previous studies, the input transfer characteristics (Id–Vg curves) of FinFET should follow the multivariate Gaussian distribution. “MultivariateNormalTril” was used to train coefficients between target variables and to improve the performance of the prediction model. It was in the last hidden layer and trained the mean vector and covariance matrix of the target variables to implement distribution. The prediction data were generated through the implemented distribution. This has been used in developing the ANN model (“Predict  $V_{th}$ ” model).



**Figure 4.** Conceptual diagram of two artificial neural networks (ANN): (1) Predict *Vth* (see top left-side one) and (2) Model *Vth* (see top right-side one). Note that two threshold voltages (*Vth,sat* and *Vth,lin*) and LER profiles ( $\sigma$ ,  $\xi_x$ , and  $\xi_y$ ) as training features are used as input for the Model *Vth*.

Two ANN models consist of four hidden layers. “ReLU” was used as the active function [18]. The “batch normalization” [19] was applied to each hidden layer, and 20% of the training sets were used as the validation data sets to prevent overfitting issues. To prevent “overfitting” in the process of developing the ANN model, the “training loss” was compared against the “val loss”. Herein, the negative log-likelihood (NLL) was used as a loss function. Note that the learning process was done using “rmsprop” as an optimizer. The number of training, i.e., epoch, was set to 5000.

To validate the model, we compared the prediction results of this study and prediction results of Simple ANN using only LER profiles as training input feature.

The ANN model was designed with the built-in functions of Keras and Python using Tensorflow2.0.

### 3. Results and Discussion

Time spent on training is summarized in Table 2. While the running time of TCAD simulation for the FinFET used in this work was ~30 min per device, the training time for the ANN models (i.e., simple ANN and this study) was up to 35 ms per epoch. TCAD simulation needs tens of hours to make one set (250 data per set), while the ANN models need a few minutes to make 10 sets (250 data per set).

**Table 2.** Time spent on training.

Model		Time
Simple ANN		450 s (15,000 epoch)
This study	Predict <i>Vth</i>	100 s (5000 epoch)
	Model <i>Vth</i>	175 s (5000 epoch)

Using the developed ANN models, the LER-induced variation of threshold voltage and others (i.e., *Vth,sat*, *Vth,lin*, *Id,sat*, *Id,lin*, *Ioff*, and *SS*) of FinFET were predicted, and then compared against the test data sets. The target variables in the test set consisting of 250 data represent the form of distribution. As previous studies have shown, the LER-induced variation of threshold voltage and others of FinFET should follow the Gaussian distribution.

Therefore, we compared the distribution of the test set against the distribution of the prediction results of the ANN models, to evaluate the model that we developed. Using the earth mover distance (EMD) score [20], the prediction performance for each model was quantitatively evaluated. Note that EMD means “the minimum amount of work required to move from one distribution to another”. EMD can be used to compare two different distributions. The EMD scores are obtained by comparing the test data (generated by TCAD) and the prediction data (generated by the simple ANN model and the prediction model suggested in this work). The EMD score shows that the prediction model in this study has better performance than the simple ANN model. Note that the values of EMD for each model are summarized in Table 3. Figure 5 shows the bar charts of the EMD by test set number, for comparison between the simple ANN model and the proposed prediction model in this study. Except for test set 6, all EMD of the proposed model in this study is lower than the simple ANN’s. Figure 6 shows the scattering plots (a–c) and box-and-whisker plots (d–i) of the 10th test set with the largest EMD gap between the simple ANN model and the prediction model suggested in this study model. We used “the Kruskal–Wallis H test” to evaluate the statistical significance. Figure 6d–i contains the  $p$ -values obtained by the Kruskal–Wallis H test of the six characteristic parameters of Id–Vg curve. The  $p$ -value as significance level was set to 0.05 in this study.

Since the ANN prediction model in this study trained the coefficient between the subthreshold features, it would accurately predict results even with relatively few data and epoch. Considering the long running-time issue in TCAD simulation, we suggest that the ANN model can be a promising alternative to TCAD simulation, when it comes to predicting the LER-induced random variation in FinFET.

**Table 3.** The EMD of each model.

	TEST SET	Amp.	Corr. x	Corr. y	EMD
Simple ANN	1	0.6248	17.0074	173.8572	0.419317
	2	0.5565	80.9191	80.5699	0.251837
	3	0.5047	48.6240	67.9938	0.208757
	4	0.5605	25.4287	69.3974	0.176496
	5	0.6373	69.1486	65.3304	0.271804
	6	0.7295	89.3916	195.6248	0.209605
	7	0.1527	23.3264	51.2533	0.178308
	8	0.6899	85.0886	80.9837	0.219300
	9	0.2593	78.1265	28.0868	0.090672
	10	0.1411	96.7100	186.6837	0.174057
	Average EMD				0.220015
This Study	1	0.6248	17.0074	173.8572	0.348625
	2	0.5565	80.9191	80.5699	0.211269
	3	0.5047	48.6240	67.9938	0.143110
	4	0.5605	25.4287	69.3974	0.161759
	5	0.6373	69.1486	65.3304	0.209351
	6	0.7295	89.3916	195.6248	0.290165
	7	0.1527	23.3264	51.2533	0.056710
	8	0.6899	85.0886	80.9837	0.112868
	9	0.2593	78.1265	28.0868	0.071807
	10	0.1411	96.7100	186.6837	0.032418
	Average EMD				0.163808

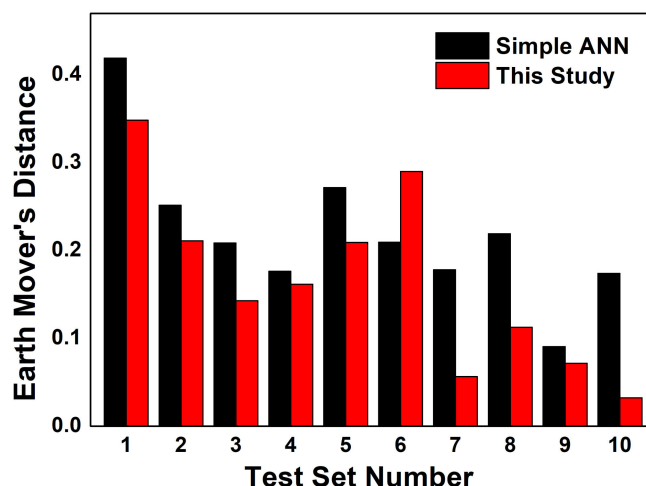


Figure 5. The earth mover distance (EMD) scores between the test sets (made by Technology Computer-Aided Design (TCAD)) and the prediction data sets (made by the simple artificial neural network (ANN) model and the prediction model suggested in this study).

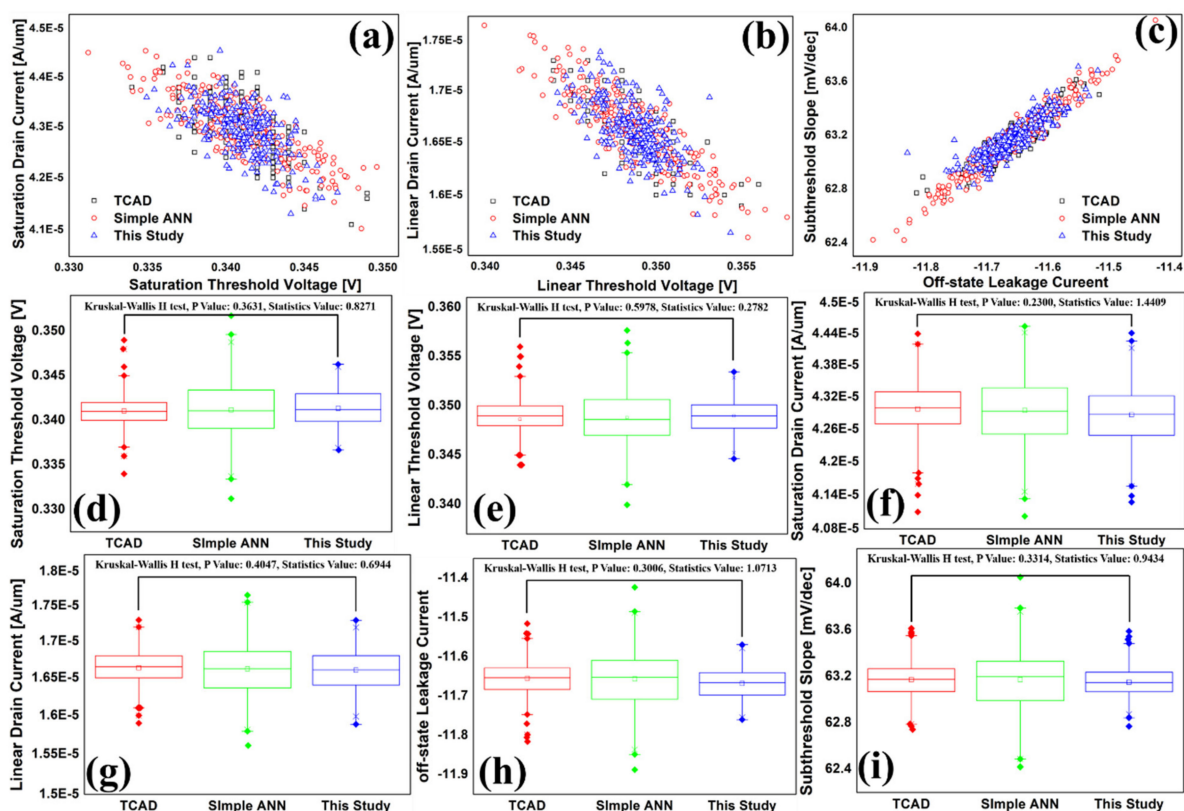


Figure 6. Scattering plots (a–c) of test data (made by TCAD) and prediction results (made by simple ANN and the ANN model proposed in this study). (d–i) Box-and-whisker plots (d–i) of electrical characteristics in  $I_d$ – $V_g$  for test data (made by TCAD) as well as for the prediction results (made by simple ANN and the ANN model proposed in this study). Note that the Kruskal–Wallis H test’s values (i.e.,  $p$ -value and statistics value) are included.

#### 4. Conclusions

We have proposed and developed an Artificial Neural Network (ANN) model to predict the LER-induced variation of the  $I_d$ – $V_g$  curve of 5 nm FinFET. The characteristic parameters of the  $I_d$ – $V_g$  curve, which are assumed to follow the Gaussian distribution, are predicted using the suggested ANN model. The model has two phases. The first is predicting the threshold voltages of two modes using LER profiles as training input

features. The second is additionally using the two threshold voltages as training input features with LER profiles to train coefficients between the subthreshold features (i.e.,  $I_{off}$ ,  $V_{th}$ , and  $SS$ ) and predicting the  $I_d$ – $V_g$  curve’s characteristics excluding  $V_{th,sat}$  and  $V_{th,lin}$  (e.g.,  $I_{off}$ ,  $I_{d,sat}$ ,  $I_{d,lin}$ , and  $SS$ ).

Comparing EMD between the test data (made by TCAD simulation) and the predicted data (made by the suggested model), we demonstrate that the predicted characteristics have very similar distributions to those of TCAD data. If the distributions of the prediction model’s results are almost similar to the distribution of the TCAD data, the prediction model has much better efficiency than TCAD simulation, in terms of simulation time (i.e., the prediction model’s training time is up to 35 ms/epoch, but the TCAD simulation running time is about 30 min/device). Thus, our ML-based prediction model has accuracy and precision as the level to TCAD simulation, and are hundreds of thousands times faster than TCAD in time.

Based on the results of this study, we suggest that the ANN prediction model based on machine learning is an effective alternative to investigate the variation induced by LER of FinFET as well as to address the time-inefficiency of the TCAD simulation.

**Author Contributions:** Conceptualization, J.L. and C.S.; methodology, J.L.; software, J.L.; validation, J.L., T.P., H.A., J.K., T.M. and C.S.; formal analysis, J.L.; investigation, J.L., T.P., H.A., and J.K.; resources, J.L.; data curation, J.L. and C.S.; writing—original draft preparation, J.L.; writing—review and editing, T.M. and C.S.; visualization, J.L.; supervision, T.M. and C.S.; project administration, T.M. and C.S.; funding acquisition, T.M. and C.S. All authors have read and agreed to the published version of the manuscript.

**Funding:** This work was supported by the National Research Foundation of Korea (NRF) grant funded by the the Korean government (MSIP) (No. 2020R1A2C1009063). This work was supported by the Future Semiconductor Device Technology Development Program (20003551) funded by the Ministry of Trade, Industry and Energy (MOTIE) and the Korea Semiconductor Research Consortium (KSRC). The EDA tool was supported by the IC Design Education Center (IDEC), Korea.

**Institutional Review Board Statement:** Not applicable.

**Informed Consent Statement:** Not applicable.

**Data Availability Statement:** Not applicable.

**Conflicts of Interest:** The authors declare no conflict of interest.

## References

- Asenov, A.; Kaya, S.; Brown, A.R. Intrinsic parameter fluctuations in decananometer MOSFETs introduced by gate line edge roughness. *IEEE Trans. Electron Devices* **2003**, *50*, 1254–1260. [[CrossRef](#)]
- Asenov, A. Random dopant induced threshold voltage lowering and fluctuations in sub-0.1/ $\mu\text{m}$  MOSFET’s: A 3-D “atomistic” simulation study. *IEEE Trans. Electron Devices* **1998**, *45*, 2505–2513. [[CrossRef](#)]
- Brown, A.R.; Roy, G.; Asenov, A. Poly-Si-gate-related variability in decananometer MOSFETs with conventional architecture. *IEEE Trans. Electron Devices* **2007**, *54*, 3056–3063. [[CrossRef](#)]
- Tsubaki, H.; Yamanaka, T.; Nishiyama, F.; Shitabatake, K. A study on the material design for the reduction of LWR. In Proceedings of the Advances in Resist Materials and Processing Technology XXIV, San Jose, CA, USA, 26–28 February 2007; p. 651918.
- Tagawa, S.; Nagahara, S.; Iwamoto, T.; Wakita, M.; Kozawa, T.; Yamamoto, Y.; Werst, D.; Trifunac, A.D. Radiation and photochemistry of onium salt acid generators in chemically amplified resists. In Proceedings of the Advances in Resist Technology and Processing XVII, Santa Clara, CA, USA, 28 February–1 March 2000; pp. 204–213.
- Prabhu, V.M.; Vogt, B.D.; Kang, S.; Rao, A.; Lin, E.K.; Satija, S.K.; Turnquest, K. Direct measurement of the in-situ developed latent image: The residual swelling fraction. In Proceedings of the Advances in Resist Materials and Processing Technology XXIV, San Jose, CA, USA, 26–28 February 2007; p. 651910.
- Constantoudis, V.; Patsis, G.; Tserapi, A.; Gogolides, E. Quantification of line-edge roughness of photoresists. II. Scaling and fractal analysis and the best roughness descriptors. *J. Vac. Sci. Technol. B Microelectron. Nanometer Struct. Process. Meas. Phenom.* **2003**, *21*, 1019–1026. [[CrossRef](#)]
- Patsis, G.P.; Constantoudis, V.; Tserapi, A.; Gogolides, E.; Grozev, G.; Hoffmann, T. Roughness analysis of lithographically produced nanostructures: Off-line measurement and scaling analysis. *Microelectron. Eng.* **2003**, *67*, 319–325. [[CrossRef](#)]
- Constantoudis, V.; Patsis, G.P.; Gogolides, E. Photoresist line-edge roughness analysis using scaling concepts. *J. Micro/Nanolithogr. MEMS MOEMS* **2004**, *3*, 429–436. [[CrossRef](#)]

10. Yamaguchi, A.; Tsuchiya, R.; Fukuda, H.; Komuro, O.; Kawada, H.; Iizumi, T. Characterization of line-edge roughness in resist patterns and estimations of its effect on device performance. In Proceedings of the Metrology, Inspection, and Process Control for Microlithography XVII, Santa Clara, CA, USA, 24–27 February 2003; pp. 689–698.
11. Bunday, B.D.; Bishop, M.; Villarrubia, J.S.; Vladar, A.E. CD-SEM measurement line-edge roughness test patterns for 193-nm lithography. In Proceedings of the Metrology, Inspection, and Process Control for Microlithography XVII, Santa Clara, CA, USA, 24–27 February 2003; pp. 674–688.
12. Wang, X.-B.; Ferris, K.; Wang, L.-S. Photodetachment of gaseous multiply charged anions, copper phthalocyanine tetrasulfonate tetraanion: Tuning molecular electronic energy levels by charging and negative electron binding. *J. Phys. Chem. A* **2000**, *104*, 25–33. [[CrossRef](#)]
13. Stewart, M.D.; Tran, H.V.; Schmid, G.M.; Stachowiak, T.B.; Becker, D.J.; Willson, C.G. Acid catalyst mobility in resist resins. *J. Vac. Sci. Technol. B Microelectron. Nanometer Struct. Process. Meas. Phenom.* **2002**, *20*, 2946–2952. [[CrossRef](#)]
14. Oh, S.; Shin, C. 3-D quasi-atomistic model for line edge roughness in nonplanar MOSFETs. *IEEE Trans. Electron Devices* **2016**, *63*, 4617–4623. [[CrossRef](#)]
15. Burke, S. Missing values, outliers, robust statistics & non-parametric methods. *Sci. Data Manag.* **1998**, *1*, 32–38.
16. Baravelli, E.; Dixit, A.; Rooyackers, R.; Jurczak, M.; Speciale, N.; De Meyer, K. Impact of line-edge roughness on FinFET matching performance. *IEEE Trans. Electron Devices* **2007**, *54*, 2466–2474. [[CrossRef](#)]
17. Chen, Y.-N.; Chen, C.-J.; Fan, M.-L.; Hu, V.P.-H.; Su, P.; Chuang, C.-T. Impacts of work function variation and line-edge roughness on TFET and FinFET devices and 32-bit CLA circuits. *J. Low Power Electron. Appl.* **2015**, *5*, 101–115. [[CrossRef](#)]
18. Bircanoğlu, C.; Arica, N. A comparison of activation functions in artificial neural networks. In Proceedings of the 2018 26th Signal Processing and Communications Applications Conference (SIU), Izmir, Turkey, 2–5 May 2018; pp. 1–4.
19. Ioffe, S.; Szegedy, C. Batch normalization: Accelerating deep network training by reducing internal covariate shift. *arXiv* **2015**, arXiv:1502.03167.
20. Rubner, Y.; Tomasi, C.; Guibas, L.J. A metric for distributions with applications to image databases. In Proceedings of the Sixth International Conference on Computer Vision (IEEE Cat. No. 98CH36271), Bombay, India, 7 January 1998; pp. 59–66.